Supporting Information

Bagher et al. 10.1073/pnas.1211946109

SI Materials and Methods

Animal Procedures and Isolated Arterial Preparation. ***Cremaster arterioles.*** Animal use was approved by the University of Oxford Local Ethical Review Committee and by the UK Home Office, and conformed to the Animals (Scientific Procedures) Act 1986. Male Wistar rats (Charles River; weight: 240–280 g) were anesthetized with urethane (2.8 g/kg i.p.), after which the cremaster muscles were exteriorized (1), excised from the rat, and placed in cool (4 °C) MOPS buffer containing (mmol/L): 145 NaCl, 4.7 KCl, 2.0 $CaCl_2$, 1.17 $MgSO_4$, 2.0 MOPS, 1.2 NaH_2PO_4, 5.0 glucose, 2.0 pyruvate, 0.02 EDTA, 2.75 NaOH (pH 7.40 ± 0.02). Following tissue removal, rats were killed following Schedule 1 procedures of the UK Animals (Scientific Procedures) Act 1986. Segments of the main intramuscular artery were dissected from the muscle as described (2, 3). Artery segments were cannulated with glass micropipettes (external diameter ~95 μm) and positioned in a 1.5-mL temperature-regulated chamber (Warner Instruments) on the stage of an inverted microscope (IX70 or IX81; Olympus) and continually superfused (2 mL·min^{-1}) with MOPS buffer. To avoid luminal flow, equal pressure was maintained across the vessel throughout experiments. Artery segments were warmed to 34 °C, gradually pressurized to 80 mmHg, longitudinally straightened (4), and allowed to develop spontaneous tone over a 20-min equilibration period. Following development of ~50% contraction/tone, arterioles were tested for leaks followed by exposure to 100 and 300 nM ACh; only arterioles dilating >95% of the Ca^{2+}-free passive diameter (maximal dilation) were used for experiments. Inner diameter was measured by using a calibrated line tool in Andor iQ (Andor Technology). Percent dilation is of maximal dilation from resting myogenic tone.

Mesenteric arteries. Male Wistar rats (Charles River; weight: 225–250 g) were killed by a Schedule 1 procedure of the UK Animals (Scientific Procedures) Act 1986. The mesentery was excised from the rat and placed in cool MOPS as described above. Segments of the third-order mesenteric artery were dissected from the surrounding fat and connective tissue as described (5). Third-order branches of rat mesenteric artery do not normally develop myogenic tone (5). Experiments were performed at 36–37 °C.

Measurement of EC and/or SMC $[Ca^{2+}]_i$ Changes in Pressurized Arterioles. ***Cell loading.*** For selective loading of the endothelium, pressurized vessels were perfused intraluminally (30 min) or bathed (120 min) at 34 °C to load the SMCs, in both cases with filtered (0.2 μm pore) MOPS-buffered solution containing Oregon Green 488 BAPTA-1 AM (OGB-1, 10 or 20 μM, respectively) and 0.0025% pluronic F-127. For simultaneous imaging of both cell types by multiphoton microscopy, ECs were loaded for the last 30 min of the SMC incubation period. In all instances, excess indicator was washed from the vessel, and the loaded AM form of the dye was allowed to de-esterify and equilibrate for at least 30 min.

Simultaneous imaging of EC and SMC Ca^{2+} events. EC and SMC fluorescence intensity was visualized by raising the focal plane to the midplane of one side of the arteriolar wall (Fig. 1*A*). Ca^{2+} responses were imaged at 40× (40×/0.9 NA objective; Olympus) by using an Olympus IX81 inverted microscope equipped with a Mai Tai DeepSee Ti:Sapphire multiphoton laser (Spectra Physics; 790 nm); images were acquired by using Olympus Fluoview 1000 software at ~3 Hz. In a 640 × 128-pixel clip box at 3× zoom, at least 1–2 ECs and 15–25 SMCs were visible. Preliminary studies showed that despite the ability to obtain equivalent fluorescence intensity images at the arteriolar midplane when using the 488-nm visible laser, the slightly higher laser intensity required caused irreversible cell damage, evidenced by focal contraction at the point of laser stimulation. To this end, all midplane experiments were performed by using a multiphoton laser, and all live cell experiments were performed with the minimal laser intensity possible to ensure contraction was not evoked.

Imaging EC or SMC Ca^{2+} events. Fluorescence intensity from selectively loaded ECs or SMCs was visualized by lowering the focal plane to the EC (Fig. 2*A*) or SMC layers at the bottom of the pressurized artery. Images were obtained by using a 40× water immersion objective (40×/0.9 NA objective; Olympus; excitation 488 nm, emission 515 nm) and captured with an iXon 887 EMCCD camera (Andor Technology) coupled to a Nipkow spinning disk confocal head (CSU22; Yokogawa), mounted on the trinocular head of the Olympus IX70 inverted microscope, and recorded using Andor iQ Software. The clip box was adjusted to allow acquisition at 8–10 Hz with at least 8–15 cells visible.

Ca^{2+} image analysis. Data were analyzed by using Metamorph software (version 7.7.4.0; Molecular Devices). For midplane experiments, regions of interest were placed on three to five active SMCs and/or one or two ECs per run, and the frequency of Ca^{2+} responses (events·cell·min^{-1}) was recorded. For SMC imaging experiments, the frequency of Ca^{2+} events for three to five active cells was averaged. Because of the rhythmicity of the SMC Ca^{2+} events, intercellular variability was low, and thus a subset of cells was chosen for analysis. For EC imaging experiments, all of the cells in the field of view (8–15 cells) were analyzed for Ca^{2+} event frequency. In all cases, only active cells were included in the average. Results are presented as frequency (events·cell·min^{-1}) or F/F_o, calculated by dividing the fluorescence (F) by an average baseline fluorescence (F_o).

Experimental Protocols. ***Effect of intraluminal pressure on EC Ca^{2+} events and diameter.*** After loading ECs with OGB-1, the vessel was equilibrated at 80 mmHg until myogenic tone developed. Intraluminal pressure was then stepwise increased between 5 and 80 mmHg. At each chosen pressure, the artery was allowed to reach steady-state diameter (~18 min) before determining the frequency of spontaneous Ca^{2+} events in ECs of pressurized arterioles.

Effect of inhibitors and vasoactive agents on EC Ca^{2+} events. The contribution of TRPV4 channels to EC Ca^{2+} events was assessed by using the selective antagonists RN 1734 (30 μM, 45- to 60-min incubation in lumen and bath) and HC 067047 (10 μM, ~70 min in bath) with the selective agonist GSK1016790A (GSK, 10–100 nM) used to demonstrate effectiveness of antagonist action. To determine the contribution of IP_3 to EC spontaneous Ca^{2+} events, arterioles were luminally perfused with the PLC inhibitor U-73122 (3 μM) or the selective inhibitor of IP_3 receptors (IP_3Rs), xestospongin C (10 μM). The contribution of voltage-gated Ca^{2+} channels (VGCC) to EC Ca^{2+} events was determined by using nifedipine (1 μM). Arterioles were incubated in the presence of ryanodine (10 μM) to assess effects of ryanodine receptor block on either EC or SMC Ca^{2+} events. The contribution of arachidonic acid was examined by blocking phospholipase A_2 (PLA_2) with AACOCF3 (3 μM).

Immunohistochemistry. Immunohistochemistry was performed in pressurized arterioles as described (5). In brief, arterioles were fixed in 2% (wt/vol) paraformaldehyde for 10 min at 37 °C, washed with PBS, and incubated in blocking buffer (luminal and abluminal, 1% BSA and 0.1% Tween 20, pH 7.1) for 60 min at 37 °C, then overnight with primary antibody at 4 °C. Primary antibodies were as follows: 1:100 rabbit polyclonal anti-rat TRPV4

(aa 853–871; Sigma, T9075); 1:100 rabbit polyclonal anti-rat $K_{Ca}3.1$ (aa 350–363; Alomone Laboratories, APC-064); 1:100 mouse monoclonal anti-human $K_{Ca}3.1$ (third extracellular loop; Alomone Laboratories, ALM-051); and 1:100 rabbit polyclonal anti-human $K_{Ca}2.3$ (aa 2–21, Alomone Laboratories, APC-025). The following day, the bath solution was replaced with PBS, and the lumen was perfused with Alexa Fluor 488 secondary antibody (1:100 goat anti-rabbit IgG, Invitrogen, A-11008; or 1:100 chicken anti-mouse IgG, Invitrogen A-21200), and incubated for 2 h at room temperature. Nuclei and elastin (including the IEL) were stained with 15 μM propidium iodide and 200 nM Alexa Fluor 633 hydrazide (Molecular Probes, A-30634), respectively (5–7). Arterioles were excited at 488, 546, and 633 nm; the fluorescence emitted at 505–525, 560–620, and 655–755nm was acquired through a water immersion objective (40×, NA 0.9, WD 0.15 mm; Olympus, 1,024 × 1,024 pixels) by using a laser scanning confocal microscope (FV1000; Olympus). z-stacks through the artery wall were obtained at 0.20-μm increments by using Fluoview Software (FV10-ASW 3.0; Olympus) and reconstructed in Imaris Software (Version 7.2.3; Bitplane).

Correlation between spontaneous Ca^{2+} events, holes in the IEL, and TRPV4 expression. In one set of experiments, arterioles were maintained at low pressure (5 mmHg), and spontaneous EC Ca^{2+} events and the IEL were imaged simultaneously at ~3 Hz by using the 488- and 633-nm visible laser lines on an Olympus FV1000 inverted microscope. Arterioles were fixed at this low pressure, and immunohistochemistry for TRPV4 channels and imaging of the stained IEL were performed, maintaining the low pressure throughout. Landmarks in the stained IEL were used to match arteriolar cellular positions directly to compare Ca^{2+} event sites (ROIs) in live tissue and TRPV4 expression in fixed tissue.

Effect of inhibitors on myogenic tone development. After initial equilibration at 80 mmHg, intraluminal pressure was dropped to 5 mmHg, then raised to 20, 40, 60, and 80 mmHg with an 18-min equilibration period between each pressure. These pressure response curves were repeated in the presence of L-NAME to block NO synthase, and then in the additional presence of RN 1734, TRAM-34, and/or apamin. RN 1734 (30 μM), TRAM-34 (1 μM), and apamin (100 nM) were used to determine the influence of TRPV4, IK_{Ca}, and SK_{Ca} channels, respectively, on the development of myogenic tone.

Drugs and Solutions. Oregon Green 488 BAPTA-1 AM (O-6807) and pluronic F-127 (P300MP) were obtained from Molecular Probes. U-73122 (BML-ST391) and xestospongin C (BML-CA409) were obtained from Enzo Life Sciences. RN 1734 (3746) and HC 067047 (4100) were from Tocris Bioscience. Apamin (L8407) was from Latoxan. All of the other drugs were provided by Sigma-Aldrich. U-73122 was dissolved in chloroform, evaporated, and then dissolved in DMSO. Xestospongin C, TRAM-34, levcromakalim, RN 1734, HC 067047, and GSK1016790A were dissolved in DMSO and then diluted in physiological buffer for experimentation (pH 7.4 at 37 °C), keeping the final DMSO concentration below 1:1,000 to avoid vehicle-associated artifacts. Glibenclamide was dissolved in ethanol. All other stock solutions were prepared in purified water. Inhibitors were added to the incubation solution, and arterioles were equilibrated for at least 15 min prior to obtaining responses if not mentioned specially.

Data Analysis. In all cases, results are summarized as the mean ± SEM of n arterioles, one per animal. Statistical comparisons were made using paired Student t test or one-way ANOVA with Bonferroni's post test as appropriate, where $P < 0.05$ was considered significant.

1. Bagher P, Segal SS (2011) The mouse cremaster muscle preparation for intravital imaging of the microcirculation. *J Vis Exp* 52):e2874.
2. McSherry IN, et al. (2006) A role for heterocellular coupling and EETs in dilation of rat cremaster arteries. *Microcirculation* 13(2):119–130.
3. Meininger GA, Zawieja DC, Falcone JC, Hill MA, Davey JP (1991) Calcium measurement in isolated arterioles during myogenic and agonist stimulation. *Am J Physiol* 261(3 Pt 2):H950–H959.
4. Kotecha N, Hill MA (2005) Myogenic contraction in rat skeletal muscle arterioles: Smooth muscle membrane potential and $Ca^{(2+)}$ signaling. *Am J Physiol Heart Circ Physiol* 289(4):H1326–H1334.
5. Dora KA, Gallagher NT, McNeish A, Garland CJ (2008) Modulation of endothelial cell $K_{Ca}3.1$ channels during endothelium-derived hyperpolarizing factor signaling in mesenteric resistance arteries. *Circ Res* 102(10):1247–1255.
6. Potocnik SJ, et al. (2009) Endothelium-dependent vasodilation in myogenically active mouse skeletal muscle arterioles: Role of EDH and $K(^{+})$ channels. *Microcirculation* 16(5): 377–390, 1, 390.
7. Clifford PS, et al. (2011) Spatial distribution and mechanical function of elastin in resistance arteries: a role in bearing longitudinal stress. *Arterioscler Thromb Vasc Biol* 31(12):2889–2896.

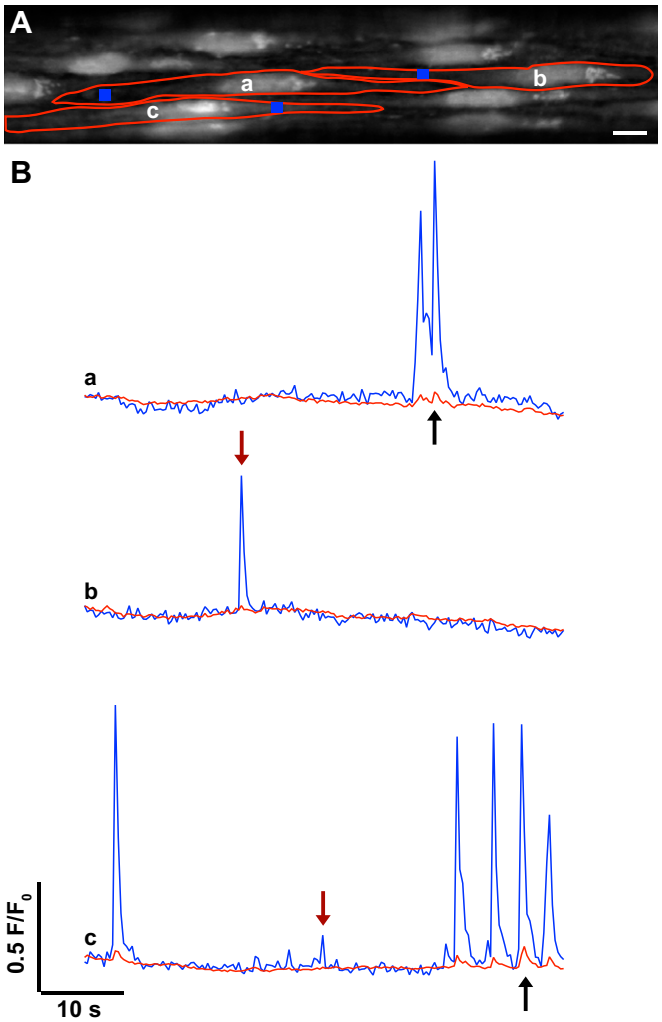

Fig. S1. Spontaneous subcellular EC Ca^{2+} events are not reflected as global EC Ca^{2+} changes in cremaster arterioles. (*A*) Ca^{2+} changes were assessed in ECs in a pressurized (to 5 mmHg) cremaster arteriole. (Scale bar, 10 μm.) Regions of interest (ROIs) were drawn around three individual ECs (a–c; red, global Ca^{2+}) and three subcellular ROIs positioned over spontaneously active sites within the same ECs (blue, subcellular Ca^{2+}). (*B*) Time-series fluorescence plots clearly demonstrate that although whole-cell ROIs (red) can detect slight changes in fluorescence during local activity (black, up arrows), these small changes do not accurately or consistently reflect the localized subcellular events (red, down arrows). *y*- and *x*-axis labels apply to each time series fluorescence plot. See Movie S2 and superimposed IEL. Acquisition rate = ~3Hz.

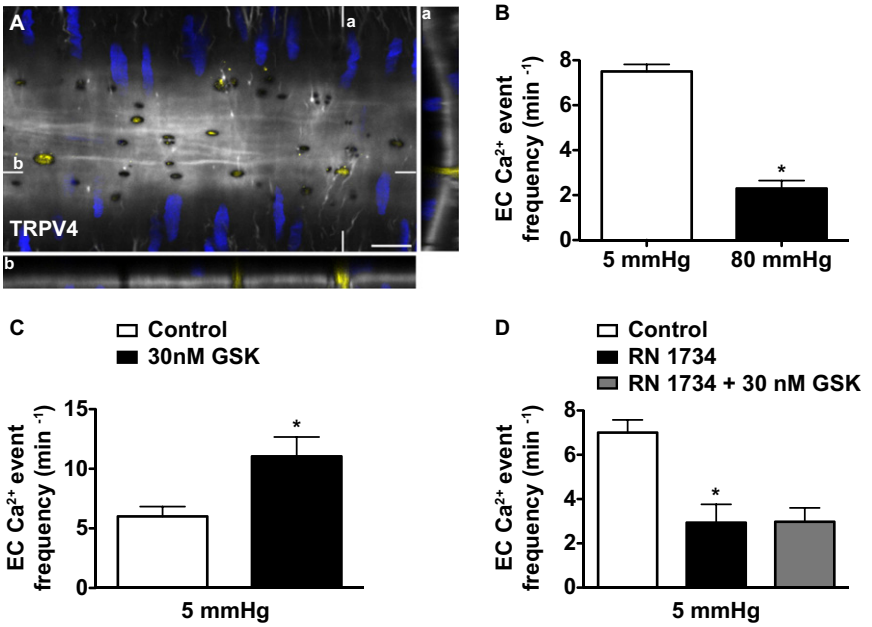

Fig. S2. Low intraluminal pressure increases EC Ca^{2+} event frequency and involves TRPV4 channels in rat mesenteric arteries that do not develop myogenic tone. (*A*) Confocal image of a pressurized mesenteric artery showing TRPV4 channel expression (yellow), elastin staining (including IEL, white), and nuclear staining (blue) (three 0.2-μm *z*-axis planes merged at the level of the IEL). Reconstructed z-stacks of the corresponding vertical plane (*a*) and horizontal plane (*b*) are indicated on the merged image in *A*. Note TRPV4 signal is primarily localized in holes through the IEL. B) The frequency of EC Ca^{2+} events at 5 mmHg was significantly greater than at 80 mmHg ($n = 3$). (*C*) GSK at a concentration of 30 nM stimulated a significant increase in EC Ca^{2+} event frequency ($n = 5$). (*D*) Summary data showing RN 1734 (30 μM) decreased the frequency of EC Ca^{2+} events at 5 mmHg ($n = 3$). *$P < 0.05$; significant difference from 5 mmHg (*B*) or control (*C* and *D*).

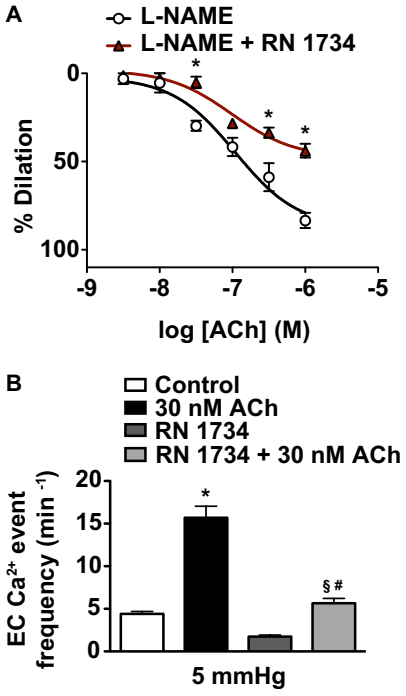

Fig. S3. The TRPV4 antagonist RN 1734 inhibits both vasodilation and EC Ca^{2+} event frequency in response to EC stimulation with ACh in cremaster arterioles. (*A*) Concentration-dependent vasodilation to ACh was significantly reduced by 30 μM RN 1734; $n = 4$. (*B*) Both spontaneous and 30 nM ACh-evoked increases in EC Ca^{2+} event frequency were reduced significantly by RN 1734 (30 μM; $n = 3$). *$P < 0.05$, significantly different from control (*A*) or L-NAME (*B*); $^{\#}P < 0.05$, significantly different from 30 nM ACh; $^{\S}P < 0.05$, significantly different from RN 1734.

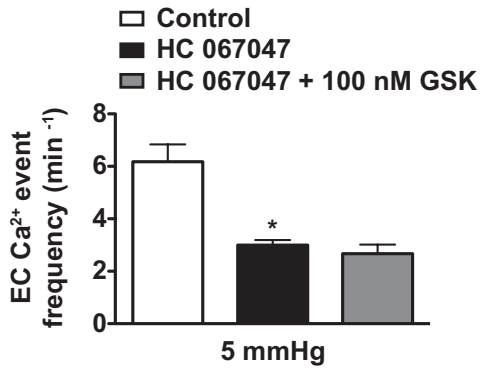

Fig. S4. The TRPV4 channel antagonist HC 067047 inhibits spontaneous Ca^{2+} activity at 5 mmHg in rat cremaster arterioles. Summary data showing HC 067047 (10 μM) decreased the frequency of EC Ca^{2+} events at 5 mmHg and prevented responses to GSK (n = 3). *P < 0.05, significant difference from control; paired experiments.

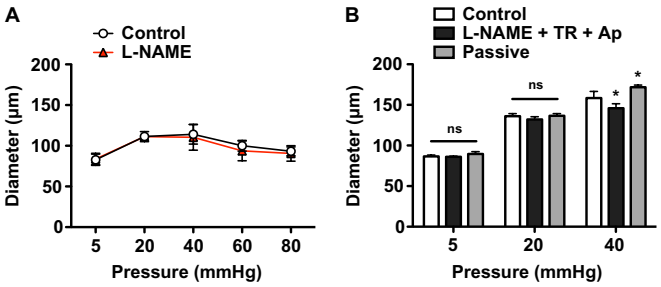

Fig. S5. Effect of nitric oxide (NO) synthase inhibition and EC disruption on myogenic tone in cremaster arterioles. (*A*) Inhibition of NO synthase with L-NAME (100 μM) had no effect on the myogenic pressure–diameter curve (n = 6). (*B*) K_{Ca} channels act through an endothelium-dependent mechanism to regulate development and maintenance of myogenic tone at low pressures. In EC denuded arterioles, TRAM-34 (TR; 1 μM, IK_{Ca} channel blocker) and apamin (Ap; 100 nM, SK_{Ca} channel blocker) did not increase myogenic tone at low pressures (5 and 20 mmHg) (n = 3). A slight but significant increase in myogenic tone was observed at 40 mmHg in the presence of TRAM-34 and apamin, but the decrease in diameter was markedly less than the same maneuver in endothelium-intact arterioles (Fig. 6). *P < 0.05, significantly different from control. ns, not significant.

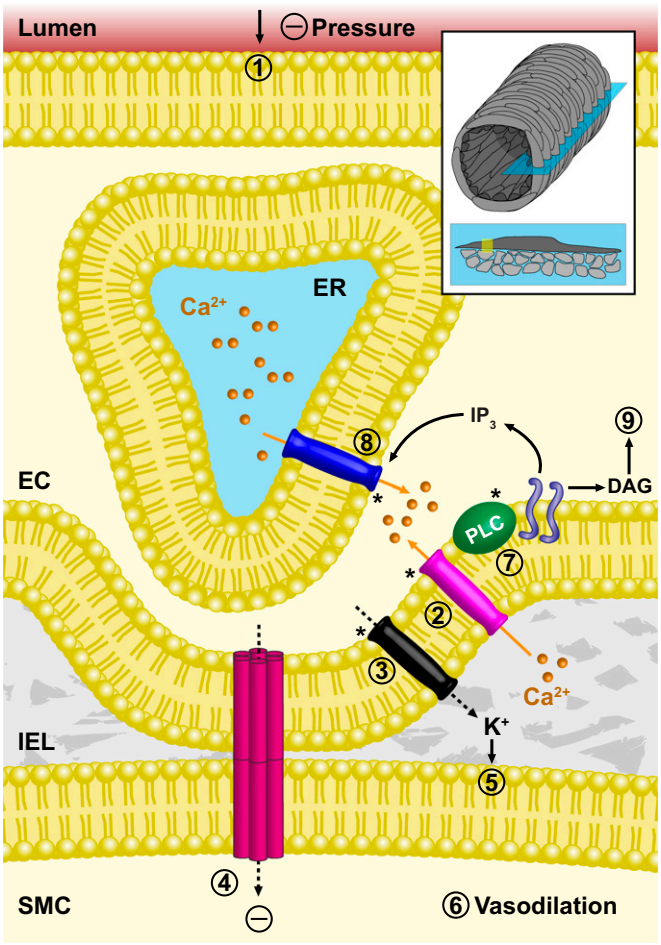

Fig. S6. Mechanisms linking low pressure, EC TRPV4 channels, and vasodilation. ECs and SMCs are separated by an IEL (see *Inset* for orientation). ECs send membrane projections through holes in the IEL where they may form heterocellular, MEJs that contribute to intercellular communication. IP_3Rs, TRPV4, IK_{Ca}, and SK_{Ca} channels are highly focused in this EC signaling "projection" microdomain. Low intraluminal pressure (1) activates Ca^{2+} influx through TRPV4 channels (2, pink). This activates EC K_{Ca} channels (3, black), hyperpolarizing the ECs, then via MEGJs (4) and diffusible endothelium-derived hyperpolarizing factors (5) the surrounding SMCs to cause vasodilation (6). In addition, PLC activity (7) liberates IP_3 and DAG. IP_3 activates IP_3Rs (8), releasing Ca^{2+} from the endoplasmic reticulum (ER) and both IP_3 and DAG activate downstream targets (9) that include TRPV4 channel complexes. Increases in Ca^{2+} can activate adjacent $[Ca^{2+}]_i$-sensitive proteins (*) amplifying Ca^{2+} events and thus vasodilation. IP_3- and TRPV4-mediated K_{Ca} activation (IK_{Ca} being most functionally relevant) occurs at low pressures (<50 mmHg), whereas IP_3-mediated events predominate at higher pressures (to 80 mmHg).

Table S1. Actions of RN 1734 at K_{ATP} channels

	Control	RN 1734	Glib	GSK	Glib + GSK
Dilation to LVK, % max	97.4 ± 1.1 (n = 4)	2.2 ± 2.2 (n = 3)	1.2 ± 1.2 (n = 4)		
EC Ca^{2+} events, min^{-1}	4.6 ± 0.4 (n = 3)	2.2 ± 0.1 (n = 4)	4.0 ± 0.2 (n = 3)	8.2 ± 0.7 (n = 3)	8.2 ± 0.7 (n = 3)

Experiments showed RN 1734 (30 μM) blocked dilation to the K_{ATP} channel opener levcromakalim (LVK; 3 μM) in a manner similar to glibenclamide (Glib; 5 μM). Arterioles were pressurized to 80 mmHg, and dilation was assessed from the resting tone. This appeared to be a nonselective effect because glibenclamide did not affect the spontaneous or GSK1016790A (GSK; 30 nM)-evoked EC Ca^{2+} events at low pressure (5 mmHg) or the myogenic tone curve (5 mmHg: control 61.3 ± 5.1, Glib 58.2 ± 4.5 μm; 80 mmHg: control 70.4 ± 9.6, Glib 63.5 ± 9.9 μm; n = 3). Thus, low pressure per se did not activate K_{ATP} channels.

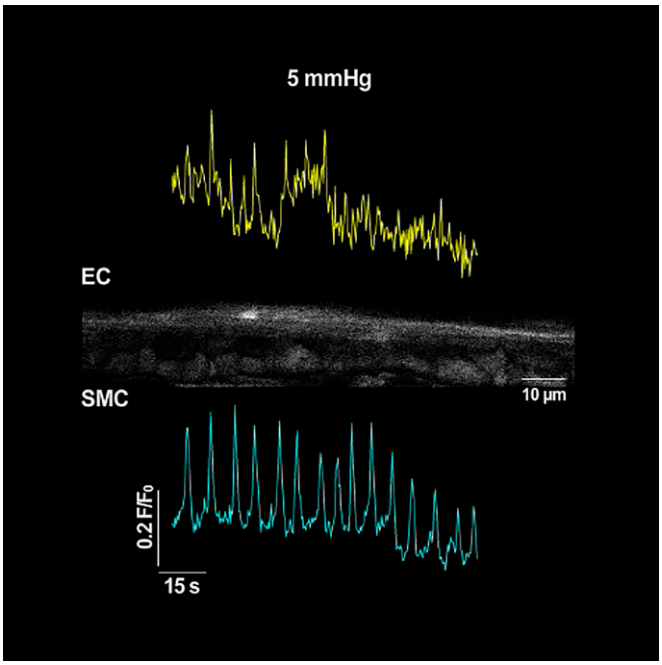

Movie S1. Simultaneous imaging of arteriolar ECs and SMCs using multiphoton microscopy. A movie of Oregon-Green BAPTA-1 loaded ECs (oriented from left to right) and SMCs (oriented perpendicular to the ECs) imaged at the midplane of an intact cremaster arteriole pressurized to 5 mmHg is shown. The first frame of the movie is a representative averaged image of the ECs and SMCs, with ROIs as indicated. The movie loops twice, with the ROIs appearing at the beginning of the second loop. Time-series plots of the calcium events in those regions of interest appear above (ECs) and below (SMCs) the movie. The movie speed is 12× real-time. (Scale bar, 10 μm.) *y*- and *x*-axis labels apply to both time-series fluorescence plots. Images were originally acquired at 0.327 s per frame.

Movie S1

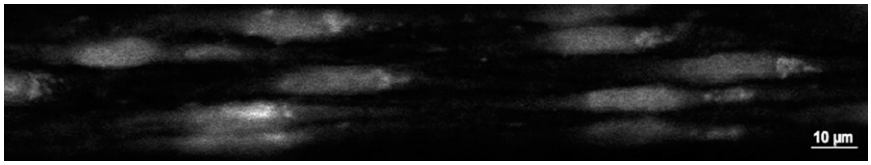

Movie S2. EC Ca^{2+} events in cremaster arterioles at 5 mmHg. Imaging of Oregon Green BAPTA-1 loaded ECs at the bottom plane of the arteriolar wall at 5 mmHg reveals local and propagating Ca^{2+} events. The movie loops twice and is played back at 12× real-time. The IEL (gold) is superimposed on the ECs, allowing for visual alignment of EC Ca^{2+} events with holes in the IEL. (Scale bar, 10 μm.) Images were originally acquired at 0.35 s per frame.

Movie S2

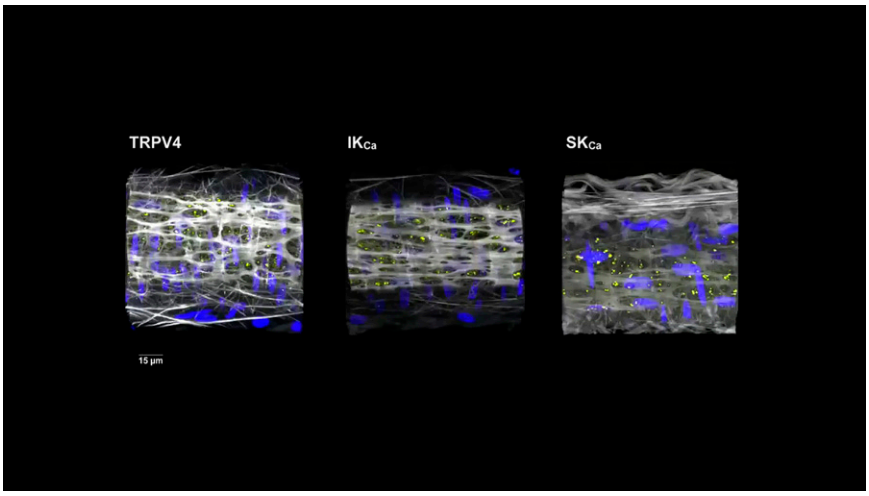

Movie S3. TRPV4, IK_{Ca}, and SK_{Ca} channels are expressed within holes in the IEL. Pressurized cannulated arterioles were fixed and stained for TRPV4 (*Left*), IK_{Ca} (*Center*), or SK_{Ca} (*Right*) channel expression. Expression of each channels is indicated in yellow (corresponding labels above each arteriole), with elastin in white and nuclear staining in blue. Note the localization of TRPV4, IK_{Ca}, and SK_{Ca} channels primarily within holes through the IEL. The *x-y* plane shows ECs orientated left to right; the vessel is rotated through 450° to show the *y–z* plane and individual *X*-stack images to visualize the alignment of channel expression with holes through the IEL. The arterioles are rotated back to the *x–y* plane, and individual *Z*-stack images shown through the vessel wall from outside to inside the lumen. (Scale bar, 15 μm, corresponding to all images.) Data are representative of results observed in three arterioles.

Movie S3